Journal of Pharmacognosy and Phytochemistry

Available online at www.phytojournal.com

E-ISSN: 2278-4136
P-ISSN: 2349-8234
JPP 2019; 8(6): 61-68
Received: 14-09-2019
Accepted: 22-10-2019

Dr. Vishal Bharat Babar
PG Research, Department of Pharmaceutical Chemistry, Dattakala College of Pharmacy, Swami-Chincholi, Tal: Daund, Dist: Pune, Maharashtra, India

Sudarshan Narayan Nagarale
PG Research, Department of Pharmaceutical Chemistry, Dattakala College of Pharmacy, Swami-Chincholi, Daund, Pune, Maharashtra, India

Prajwala Rajkumar Khapale
Department of Pharmacology and Toxicology, Dattakala College of Pharmacy, Swami-Chincholi, Daund, Pune, Maharashtra, India

Corresponding Author:
Dr. Vishal Bharat Babar
PG Research, Department of Pharmaceutical Chemistry, Dattakala College of Pharmacy, Swami-Chincholi, Tal: Daund, Dist: Pune, Maharashtra, India

Biosynthesis of silver nanoparticles of aqueous extract of *plectranthus amboinicus* (lour.) Spreng for anticancer activity

Dr. Vishal Bharat Babar, Sudarshan Narayan Nagarale and Prajwala Rajkumar Khapale

Abstract
Present studies, silver nanoparticles (AgNPs) were biosynthesized using aqueous extract of *Plectranthus amboinicus (Lour.) Spreng* plant. The prepared AgNPs (PA-AgNPs) were examined by Ultraviolet-visible spectroscopy, Fourier transform infrared (FTIR) spectroscopy, X-ray diffraction (XRD), Transmission electron microscopy (TEM), Scanning electron microscope (SEM), and Energy dispersive spectroscopy (EDX). The results obtained from various characterizations revealed that average size of biosynthesized AgNPs was 33 nm and in face-centered-cubic structure. The anticancer potential of PA-AgNPs was investigated against Human cervical cancer cells (HeLa). The cytotoxic response was assessed by MTT assay and NRU assays. Further, the influence of cytotoxic concentrations of PA-AgNPs cell cycle arrest and apoptosis/necrosis was studied. The cytotoxic response observed was in a concentration-dependent manner. The cell cycle analysis and apoptosis/necrosis assay data exhibited PA-AgNPs-induced SubG1 arrest and apoptotic/necrotic cell death. The biosynthesized AgNPs-induced cell death in HeLA cells suggested the anticancer potential of PA-AgNPs to treat the cervical cancer cells.

Keywords: *Plectranthus amboinicus (Lour.) Spreng*, Biobiosynthesis, Silver Nanoparticles, HeLa, Anticancer etc.

Introduction
Nobel metal nanoparticles have attracted the interest of scientific community due to their fascinating applications in the field of biology, material science, medicine, etc. [1]. Silver nanoparticles specifically have gained attention due to their unusual physiochemical [2] (chemical stability and electrical conductivity) and biological activities such as antibacterial, antifungal, anti-inflammatory, antiviral, antiangiogenesis, anticancer, and antiplatelet activities [3–5]. In addition, silver nanoparticles have been used in clothing [6], room spray, laundry detergent, wall paint formulation [7, 8], sunscreens, and cosmetics [9]. Silver nanoparticles also inhibit HIV-1 virus from binding to the host cells *in vitro* [10]. Although a wide variety of metal nanoparticle preparation methods such as UV radiation, laser ablation, lithography, aerosol technologies, and photochemical reduction are available [11–13], The focus is shifting towards biosynthesis of nanoparticles, using bacteria [14], yeast [15], fungi [16], and plants [17]. Biosynthesis of nanoparticles reports to be clean, nontoxic, cost effective, and environmentally benign. Among The various biological methods available, the use of microbe-mediated biosynthesis has limited industrial use, as they require antiseptic conditions. On The contrary, the use of plant extract for the nanoparticles biosynthesis is valuable due to the ease of scaleup, less biohazardous nature, and avoiding the hideous procedure of maintaining the cell lines [18].
Cancer is a life threatening disease and leads The cases of deaths around the world [19]. According to the WHO, the annual cancer cases are to rise from 14 million in 2012 to 22 million in the next two decades [20]. Thus, the development of potent and effective antineoplastic drugs is one of the most persuaded goals. Among the various approaches, the exploitation of natural products is one of the most successful methods to identify novel hits and leads [21]. *Plectranthus amboinicus* (Lour.) Spreng. (Lamiaceae) is a medicinal plant growing in rural parts of India [22]. Traditionally *P. amboinicus* was used as a sedative; The leaf decoction was drunk with tea to release stomach and burn problems [23, 24]. The antimicrobial, anticancer, and antioxidant activities of *P. amboinicus*are documented [25]. Recently, we have reported the positive effects of *P. amboinicus* on human breast and lung cancer cell lines [26]. However, until the present, no published data are available on biosynthesis of nanoparticles using *P. amboinicus* plant. Herein, we report for the first time silver nanoparticles (PA-AgNPs) biosynthesis through a single step silver ions reduction by *P.*

amboinicus plant extract (Figure1) and studied the anticancer activity of the biosynhesized silver nanoparticles against human cervical cancer (HeLa) cells.

Materials and Methods

Plant Material, Reagents, and Consumables

Plectranthus amboinicus (Lamiaceae) plants were collected from the rural area of Bhigwan, Pune District, Maharashtra. The specimen sample was taxonomically identified and authenticated by the Department of Botany, Dattakala School and Jr. College, Swami-Chincholi, where a voucher specimen was deposited (authentication no. DKJrCBL No. 2019145). Cell culture medium, antibiotics-antimycotic solution, and trypsin procured from IIV, Pune and KLE University, Belgavi. Plastic wares and other consumables were obtained from Scienty Lab, Mumbai. Other chemicals/reagents used in this study were purchased from Yarrow Labs, Mumbai.

Preparation of Plant Extract

The aerial part of *P. amboinicus*was collected and washed several times with distilled water to remove dust and was dried under shade. The air-dried plant was cut into small pieces, macerated in distilled water, filtered under gravity, and the solvent evaporated under reduced pressure using a rotary evaporator. The dried extract was kept at 4°C (Figure1).

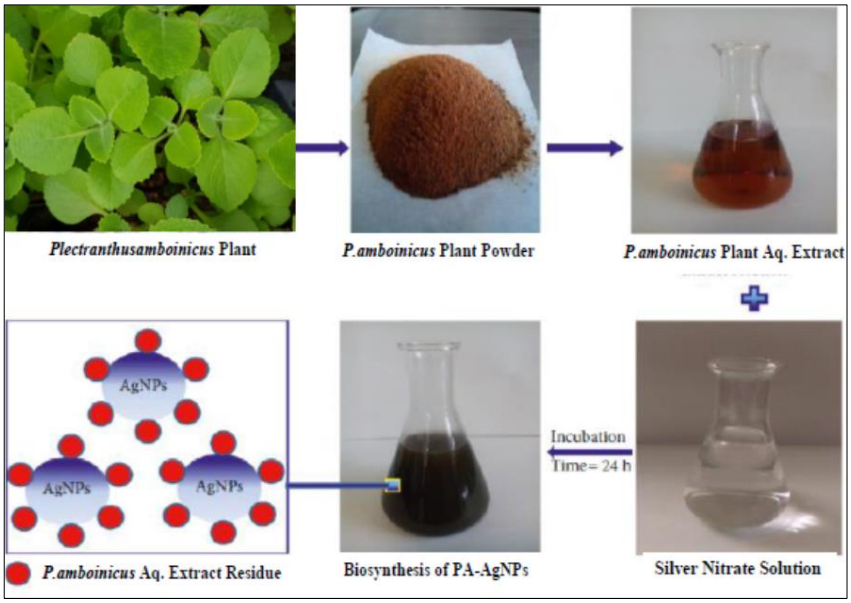

Fig 1: Schematic illustration of the biosynthesis of silver nanoparticles (PA-AgNPs) using aqueous extract of the *Plectranthus amboinicus* plant.

Biosynthesis of Silver Nanoparticles

The aqueous extract of *P. amboinicus* (500 mg) was dissolved in 100 ml distilled water. Further 10 ml of the above extract was added to 90 ml of 0.1 M AgNO3 solution. After 24 h incubation, the solution turned dark brown, which indicates the formation of AgNPs. The solution was then transferred into a round bottom flask and was heated with continuous stirring at 90°C. After 15 min, the centrifugation was done at room temperature and a speed of 9000 rpm. The black powder obtained after washing thrice with distilled water was dried overnight in an oven at 80° C.

Characterization of Biosynthesized Silver Nanoparticles:

The optical absorption of synthesized silver nanoparticles was studied using FTIR (Shimadzu FT-IR Prestige 21) and UV-VIS (Shimadzu UV-VIS 2550, Japan) spectral analysis, respectively. Fourier transmission infrared (FTIR) spectra were recorded using KBr pellets in the range of 4000 to 400 cm−1. The crystalline nature of synthesized AgNPs was confirmed by XRD pattern. The XRD data were recorded using PAN alytical X'Pert X-ray diffractometer using CuKα (λ = 1.54056 A˚). Morphology, size, and electron diffraction pattern were examined by SEM (JSM-7600F, Japan) and TEM (JEM2100F, Japan) at a voltage 200 kV, respectively. EDX analysis was used to confirm the presence of elemental silver in synthesized AgNPs.

Cytotoxicity by MTT Assay

Cytotoxicity of PA-AgNPs was examined by using MTT assay according to the method in [27]. In brief, HeLA cells obtained from KLE University, Belgavi were plated in 96-well plates at a density of 1 x 104 cells / well. Cells were exposed to 1–100µg/ml PA-AgNPs for 24 h. Following this, MTT was added in the wells, and plates were incubated for 4 h further. The reaction mixture was taken out and 200 µl/well DMSO was added and mixed several times by pipetting up and down. The absorbance of plates was measured at 550 nm. The results were expressed as percentage of control.

Cytotoxicity by Neutral Red Uptake (NRU) Assay

Cytotoxicity by NRU assay was performed using the procedure [27]. Briefly, HeLA cells were treated with 1–100 µg/ml PA-AgNPs for 24 h. Then, cells were washed with PBS twice and incubated further in 50 µg/ml of neutral red containing medium for 3 h. The cells were washed off with a solution (1% CaCl2 and 0.5% formaldehyde). The dye was extracted in a mixture of 1% acetic acid and 50% ethanol. The plates were measured at 550 nm. The results were expressed as percentage of control [28-29].

Cell Cycle Analysis

PA-AgNPs-induced changes in cell cycle were measured using the protocol [30]. In brief, HeLa cells were exposed for 24 h at 10–50 µg/ml PA-AgNPs. After the treatment, cells were fixed in chilled 70% ethanol for 1 h. Then, cells were washed twice by centrifugation, and cells were stained with propidium iodide for 60 min in dark. The stained cells were acquired by flow cytometer.

Apoptosis Assay

The apoptosis/necrosis induced by PA-AgNPs in HeLA cells were analysed using Annexin-V and 7- AAD Kit (Beckman Coulter) following the manufacturer's protocol. The amount of apoptosis/necrosis in the treated HeLa cells was analysed by flow cytometry following the protocol [31].

Statistical Analysis

Data were statistically analysed by ANOVA using the post hoc Dunnett's test. Value $p < 0.05$ was considered as a significant level between the exposed and control sets. The results are presented as mean ± standard deviation of three experiments.

Result and Discussion

Biosynthesis and Characterization of PA-AgNPs

Plant aqueous extract of *P. amboinicus* was used for the biosynthesis of PA-AgNPs under facile conditions. The colorless silver nitrate solution (Figure1) turned dark brown indicating the formation of silver nanoparticles (AgNPs). The occurrence of brown color can be attributed to the surface plasmons [32], arising from the collective oscillations of valance electrons in the electromagnetic field of incident radiation. Figure2 (a) shows the UV-V is spectra of the biosynthesized AgNPs, giving the plasmon resonance at 400 nm. The characteristic λ max for AgNPs is in the range of 400–500 nm [33]. The position and shape of the surface plasmon absorption is dependent on the shape and size of particles formed, their interparticle distance, and the dielectric constant of the surrounding medium [34, 35]. Similar observations are reported earlier [32, 36].

FTIR measurements were carried out to identify the various functional groups in biomolecules responsible for the reduction of silver ions to AgNPs and capping/stabilization of AgNPs. The band intensities in different region of spectra for *P. amboinicus* extract Figure2 (b) and biosynthesized silver nanoparticles Figure2(c) were analysed. The similarities between the two FTIR spectra, with some marginal shifts in peaks clearly indicate the plant extract is also acting as a capping agent. The *P. amboinicus* plant extract showed a number of peaks reflecting a complex nature of the plant extract. The shift in peaks at 3426 cm^{-1} corresponding to NH stretching of amide (II) band or C-O stretching or O-H stretching vibration implicated that their groups may be directly involved in the process of biosynthesis of AgNPs.

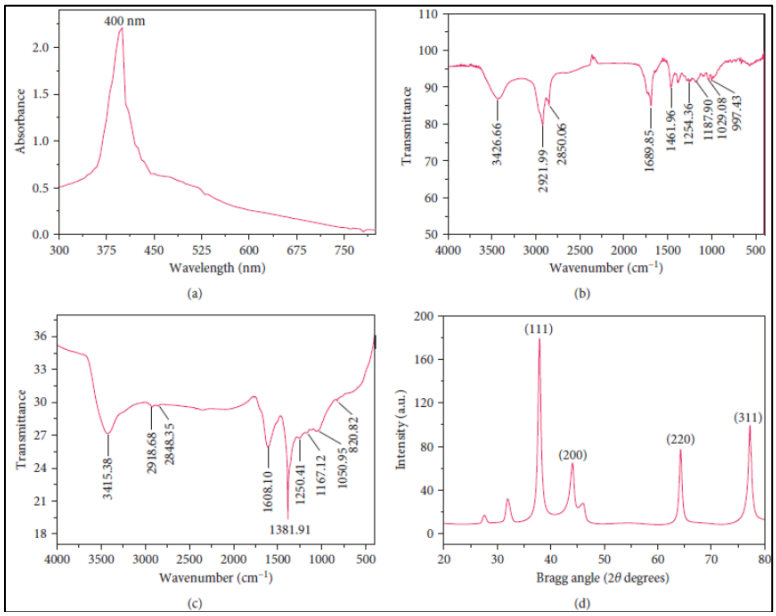

Fig 2: Characterization of biosynthesized silver nanoparticles (PA-AgNPs) prepared using aqueous extract of The *Plectranthus amboinicus* plant. (a) Ultraviolet-visible absorption spectra of biosynthesized silver nanoparticles (AgNPs). (b) Fourier-transform infrared spectra of *P. amboinicus* extract. (c) Fourier-transform infrared spectra of biosynthesized silver nanoparticles (PA-AgNPs). (d) X-ray powder diffraction pattern of biosynthesized silver nanoparticles (PA-AgNPs).

Further, peak shifts from 1689 cm^{-1} to 1608 cm^{-1} indicated the possible involvement of C=O stretching or C-N bending in the amide group. Besides, the peak shifts from 1461 cm^{-1} to 1381 cm^{-1} suggest the involvement of C-H or O-H bending vibration of methyl, methylene, or alcoholic group in the reduction of Ag. Moreover, the observed peaks are more characteristic of flavonoids and terpenoids [37] that are present in the *P. amboinicus* species [25, 26]. It could be speculated that these secondary metabolites are responsible for the biosynthesis/stabilization of PA-AgNPs.

The crystalline structure of the biosynthesized AgNPs was determined by XRD technique. Figure2 (d) displays The XRD pattern of synthesized AgNPs. The Bragg reflection with 2θ values of 37.89, 44.23, 64.26, and 77.24 corresponding to (111), (200), (220), and (311) sets of lattice planes, respectively, is observed. These can be indexed to the face centered cubic (fcc) structure of the biosynthesized AgNPs. The crystalline size of the AgNPs was determined by using Debye–Scherrer equation [38]:

$$D = 0.9\lambda / \beta \cos \theta \ldots\ldots\ldots (1)$$

Where D is the grain size, λ is the wavelength of X-ray (1.54056A), and ˚ β is the full width at half maxima of the diffraction peak (in radians).

The average grain size determined by broadening of (111) reflection is estimated to be around 33 nm. Similar results have been reported earlier [39]. The absence of any reflection other than belonging to the silver lattice clearly indicates that the biosynthesized AgNPs lattice was unaffected by other molecules in the extract of plant. The scanning electron microscopy (SEM) and transmission electron microscopy (TEM) was employed to study the morphological and structural features of biosynthesized AgNPs.

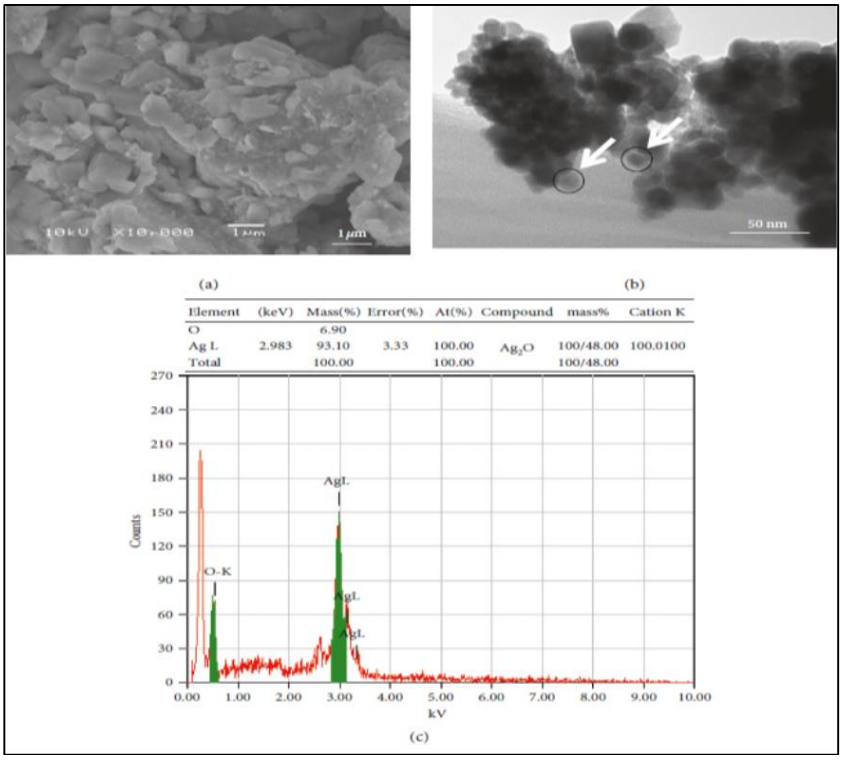

Fig 3: (a) SEM image of the biosynthesized silver nanoparticles (AgNPs); (b) TEM image of biosynthesized silver nanoparticles (PA-AgNPs) at 50 nm; (c) energy-dispersive X-ray spectrum of biosynthesized silver nanoparticles (PA-AgNPs).

The SEM image Figure3 (a) shows that relatively spherical and uniform nanoparticles are formed. Some of the larger particles seen may be due to aggregation of nanoparticles induced by evaporation of solvent during sample preparation [40]. The TEM image Figure3 (b) revealed the nanoparticles formed have a narrow size distribution. The average size was about 33 nm, supporting the results of XRD further. Further, the energy-dispersion X-ray (EDX) spectroscopy study was employed to detect the existence of elemental silver. Figure3 (c) shows the EDX image of *P. amboinicus* biosynthesized AgNPs. The results clearly indicate an intense signal at approximately 2.98 KeV corresponding to the presence of metallic silver nanocrystals, occurring due to surface plasmon resonance (SPR) [41]. The other intense signal at around 0.0–0.5 Kev represents the characteristic absorption for oxygen and carbon. This indicates the presence of *P. amboinicus* plant extract as a capping ligand on the surface of AgNPs.

Cytotoxicity Assessments of PA-AgNPs by MTT and NRU Assays:

The key results obtained by MTT and NRU assays in HeLA cells exposed to 1 µg/ml to 100µg/ml for 24 h are summarized in Figure4 (A) and 4(B).

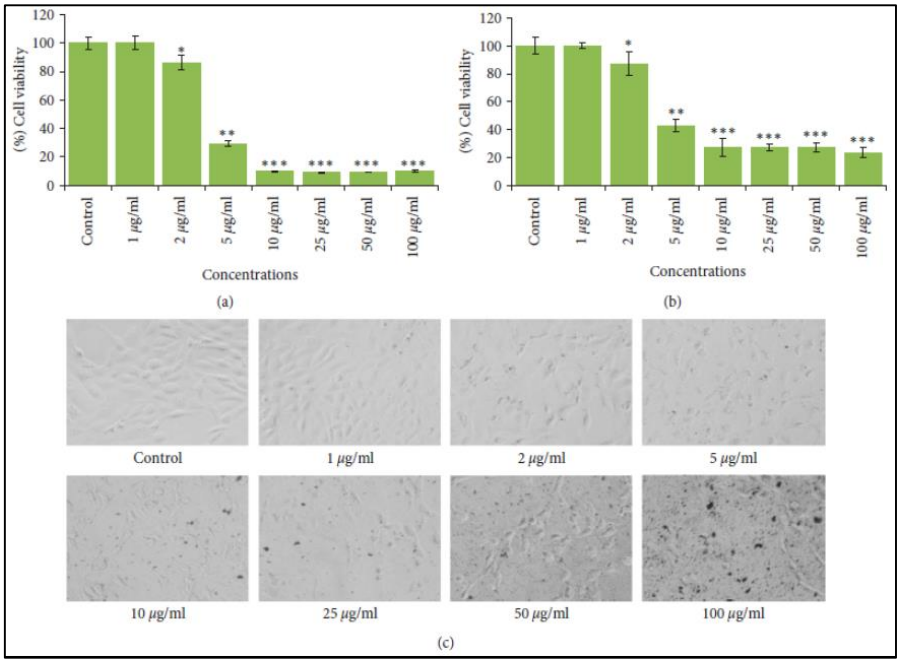

Fig 4: Cytotoxicity assessment in HeLA cells following the exposure of various concentrations of PA-AgNPs for 24 h: (a) MTT assay; (b) neutral red uptake assay. (c) Morphological changes. Images were taken using an inverted phase contrast microscope at 20x magnification. $*p < 0.05$, $**p < 0.01$, $***p < 0.001$ vs control.

The results exhibited a concentration dependent decrease in the viability of HeLA cells. The cell viability was recorded as 86% and 29% in PA-AgNPs at 2 µg/ml and 5 µg/ml concentrations, respectively; however, the maximum decrease in cell viability was measured as 9% each at 10, 25, 50, and 100 µg/ml of PA-AgNPs Figure4 (A). Like MTT assay, a concentration-dependent decrease in cell viability of HeLA cells exposed to PA-AgNPs was also observed by NRU assay. The cell viability was recorded as 87% and 43% in PA-AgNPs at 2 µg/ml and 5 µg/ml concentrations, respectively; however, the maximum decrease in cell viability was measured as 23% at 100 µg/ml of PA-AgNPs Figure4 (B). In this study, the cytotoxicity assessments were performed using two independent end points (MTT and NRU) assays [42]. The MTT, a colorimetric assay is based on the mitochondrial dehydrogenase enzyme of viable cells [43]; however, NRU assay is based on the lysosomal integrity of viable cells [44]. The cytotoxic responses of the PA-AgNPs, suggesting that biosynthesized AgNPs could contribute in search of alternative chemotherapeutic agent. Our results showed more than 50% of cell death even at 5µg/ml of PA-AgNPs. The cytotoxic effects induced by PA-AgNPs at lower concentrations could be due to the plant components attached to the AgNPs [45]. The results obtained from this study are also very well supported with various evidences for the cytotoxic effect of biosynthesized AgNPs using *Annona squamosa* leaf extract against the breast cancer MCF-7 cell line [46], *Piper longum* leaf extracts against Hep-2 cancer cell line [47], and *Morinda citrifolia* against HeLa cell lines [48-51] *in vitro*.

Cell Cycle Analysis

The results of cell cycle analysis in HeLA cell lines exposed to PA-AgNPs at 10–50 µg/ml for 24 h are represented in Figure5.

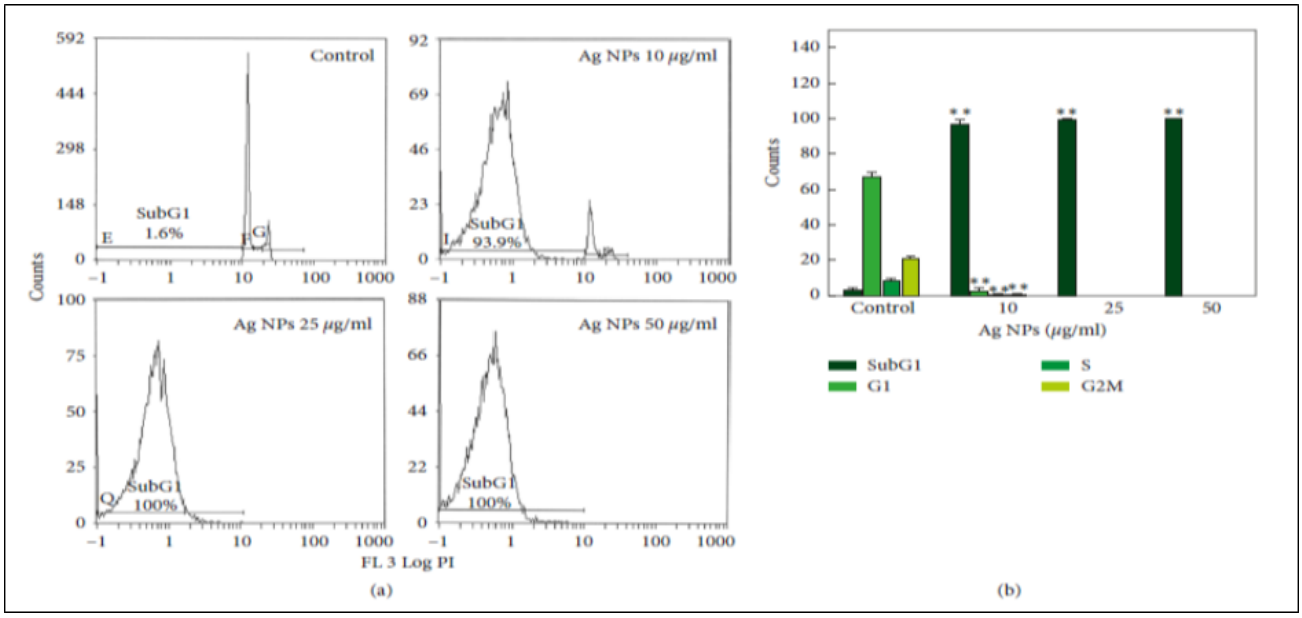

Fig 5: Cell cycle analysis in HeLA cells exposed to 10–50 µg/ml concentrations of PA-AgNPs for 24 h. (a) Representative flow cytometric image exhibiting changes in the progression of cell cycle. SubG1 in each micrograph represents the percentage of cells in the SubG1 phase. (b) Each histogram represents the percentage of cells arrested in different phases of cell cycle. Results are expressed as the mean ± S.D. of three independent experiments. $^{**}p < 0.001$ vs control.

The flow cytometric measurement of propidium iodide-stained control and PA-AgNPs-treated HeLA cells showed an increase in apoptotic SubG1 peak. A significant increase in SubG1 arrest was observed at 50 µg/ml concentrations of PA-AgNPs-treated HeLA cells (Figure5). The increase in the SubG1 (apoptotic) population found in this study suggests that PA-AgNPs-treated HeLA cells were not able to go through G2 checkpoint; therefore, G2/M transition was found to be affected. The apoptosis induction due to the presence of SubG1 peak in the process of cell cycle suggests the role of early and late apoptotic/necrotic pathway [52-57].

Apoptosis Assessment Using Annexin V-PE and 7-AAD:

The results obtained from the induction of apoptosis using flow cytometry are summarized in Figure 8. The flow cytometry data clearly showed that PA-AgNPs induced cell death in HeLA cells. Based on the Annexin V-PE/7-ADD staining, 94.2% of HeLA control cells were found alive with values of 0.56%, 3.31%, and 1.9% of cells, which are normal process for cells growing in cultures.

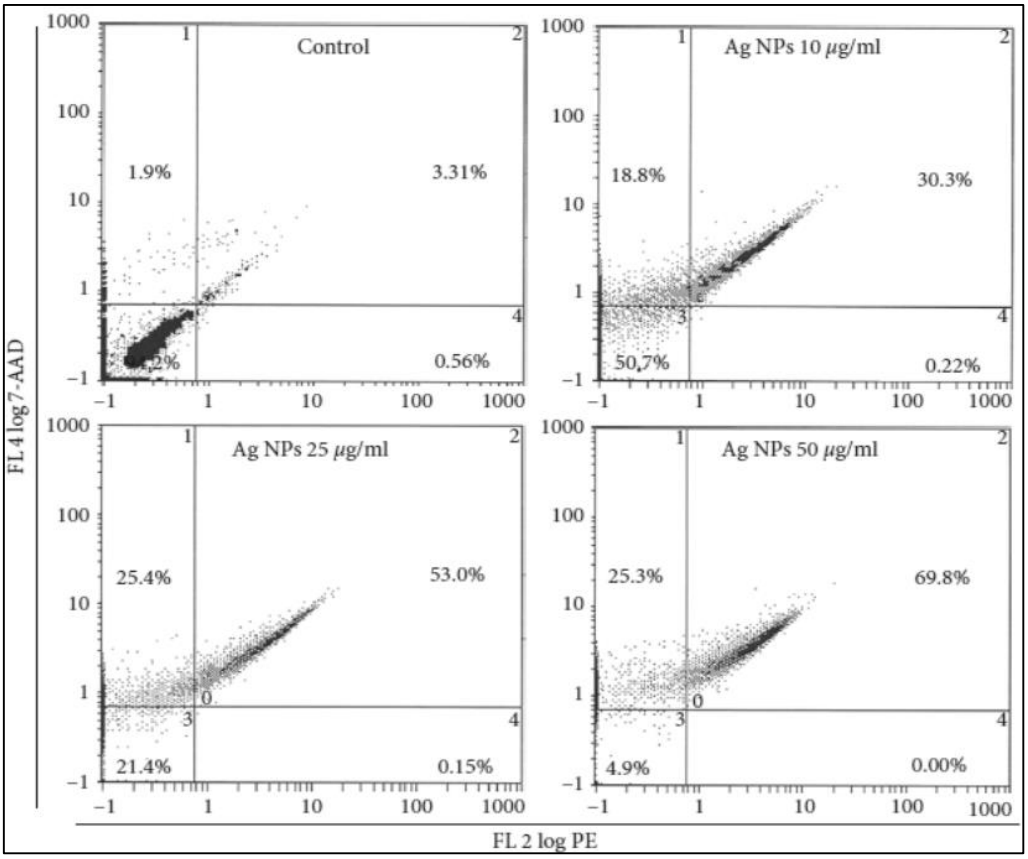

Fig 6: Annexin V-PE (phycoerythrin) and 7-AAD (7-amino actinomycin D assay. Bivariate flow cytometry analysis of HeLA cells treated with different concentrations of PA-Ag NPs. The scatter plots show early apoptotic, late apoptotic, and necrotic cells following 24 h treatment.

The HeLA cells exposed to PA-AgNPs significantly increased the late apoptotic and necrotic cells as compared with untreated control cells. An increase in the percentage of apoptotic and necrotic cells was found with the values of 30.3–69.8% and 18.8–25.3% between 10 µg/ml and 50 µg/ml PA-AgNPs concentrations, respectively (Figure6). Even at lower concentration, i.e., 10µg/ml, PA-AgNPs were found to induce apoptotic and necrotic cell death. It is well known that high amount of ROS generation could lead to apoptotic and necrotic cell death [58]. The excessive ROS generation has been linked with the substantial DNA damage and apoptosis [59]. Our results are in well accordance with the recent reports that have shown apoptosis cell death due to the exposure of nanoparticles [60], including the exposure of plant-synthesized silver nanoparticles [52].

Conclusions

This investigation demonstrated the biosynthesis of silver nanoparticles (AgNPs) for the first time, via a single-step reduction of silver ions using *Plectranthus amboinicus* plant and its anticancer potential against human cervical cancer (HeLa) cells. Our results showed that biosynthesized AgNPs (PA-AgNPs) induced a concentration-dependent cytotoxicity in HeLA cells. This study also showed that PA-AgNPs have the capacity of inducing apoptosis and necrosis cell death of HeLA cells through SubG1 cell cycle arrest. Thus, our findings suggest the anticancer potential of biosynthesized PA-AgNPs against human cervical cancer cells and could play an important role in the development of new therapeutic agent for the treatment of cancer.

References

1. Yokohama K, Welchons DR. "The conjugation of amyloid beta protein on the gold colloidal nanoparticles surfaces," Nanotechnology 2007;18(10):105101-105107.
2. Sharma VK, Yngard RA, Lin Y. "Silver nanoparticles: Biosynthesis and their antimicrobial activities," Advances in Colloid and Interface Science 2009;145(1-2):83-96.
3. Wong KK, Liu X. "Silver nanoparticles—the real "silver bullet" in clinical medicine," Med Chem Comm, 2010;1(2):125-131.
4. Monteiro DR, Silva S, Negri M *et al*., "Silver nanoparticles: influence of stabilizing agent and diameter on antifungal activity against Candida albicans and Candida glabrata biofilms," Letters in Applied Microbiology 2012;54(5):383-391.
5. Krishnaraj C, Ramachandran R, Mohan K, Kalaichelvan PT. "Optimization for rapid biosynthesis of silver nanoparticles and its effect on phytopathogenic fungi," Spectrochimica Acta Part A: Molecular and Biomolecular Spectroscopy 2012;93:95-99.
6. Mart´ınez-Gutierrez F, Thi EP, Silverman JM *et al*., "Antibacterial activity, inflammatory response, coagulation and cytotoxicity effects of silver nanoparticles," Nanomedicine: Nanotechnology, Biology and Medicine 2012;8(3):328-336.
7. Gottesman R, Shukla S, Perkas N, Solovyov LA, Nitzan Y, Gedanken A. "Sonochemical coating of paper by microbiocidal silver nanoparticles," Langmuir 2011;27(2):720-726,.
8. Os´orio I, Igreja R, Franco R, Cortez J. "Incorporation of silver nanoparticles on textile materials by an aqueous procedure," Materials Letters 2012;75:200-203.
9. Martinez-Gutierrez F, Olive PL, Banuelos A *et al*., "Biosynthesis, characterization, and evaluation of antimicrobial and cytotoxic effect of silver and titanium nanoparticle," Nanomedicine 2010;6(5):681-688.

10. Favero J, Corbeau P, Nicolas M *et al*., "Inhibition of human immunodeficiency virus infection by the lectin jacalin and by a derived peptide showing a sequence similarity with gp120," European Journal of Immunology 1993;23(1):179-185.
11. Okitsu K, Yue A, Tanabe S, Matsumoto H, Yobiko Y. "formation of colloidal gold nanoparticles in an ultrasonic field: control of rate of gold (III) reduction and size of formed gold particles," Langmuir 2001;17(25):7717–7720.
12. Naik RR, Stringer SJ, Agarwal G, Jones SE, Stone MO. "Biomimetic biosynthesis and patterning of silver nanoparticles," Nature Materials 2002;1(3):169-172.
13. Narayanan KB, Sakthivel N. "Biological biosynthesis of metal nanoparticles by microbes," Advances in Colloid and Interface Science 2010;156(1-2):1-13.
14. Mandal D, Bolander ME, Mukhopadhyay D, Sarkar G, Mukherjee P. "The use of microorganisms for the formation of metal nanoparticles and their application," Applied Microbiology and Biotechnology 2006;69(5):485-492.
15. Kowshik M, Ashtaputre S, Kharrazi S *et al*., "Extracellular biosynthesis of silver nanoparticles by a silver-tolerant yeast strain MKY3," Nanotechnology 2002;14(1):95-100.
16. Mukherjee P, Ahmad A, Mandal D *et al*., "Fungus-mediated biosynthesis of silver nanoparticles and their immobilization in the mycelial matrix: a novel biological approach to nanoparticle biosynthesis," Nano Letters, 2001;1(10):515-519.
17. Iravani S. "Biosynthesis of metal nanoparticles using plants," Chemistry 2011;13(10):2638-2650.
18. Kalishwaralal K, Deepak V, Pandian SRK *et al*., "Biobiosynthesis of silver and gold nanoparticles using Brevi bacteriumcasei," Colloids and Surfaces B: Biointerfaces 2010;77(2):257-262.
19. Gao X, Lu Y, Fang L *et al*., "Biosynthesis and anticancer activity of some novel 2-phenazinamine derivatives," European Journal of Medicinal Chemistry 2013;69:1-9.
20. McGuire S. "World cancer report 2014. Geneva, Switzerland: world health organization, international agency for research on cancer, WHO press, 2015," Advances in Nutrition 2016;7(2):418-419.
21. Newman DJ, Cragg GM. "Natural products as sources of new drugs over the 30 years from 1981 to 2010," Journal of Natural Products 2012;75(3):311-335.
22. Rahman MA, Mossa JS, Al-Said MS, Al-Yahya MA. "Medicinal plant diversity in the flora of India1: a report on seven plant families," *Fitoterapia* 2004;75(2):149-161.
23. Mossa JS, Al-Yahya MA, Al-Meshal IA. Medicinal Plants of Saudi Arabia, King Saud University Press, Riyadh, Saudi Arabia, 2000.
24. Hedge C. "Studies in the flora of Arabia 2, some new and interesting species of *labiatae*," Notes from the Royal botanic Garden Edinburgh 1982;40(2):63-74.
25. Mothana RA, Gruenert R, Bednarski PJ, Lindequist U, "Evaluation of the *in vitro* anticancer, antimicrobial and antioxidant activities of some Yemeni plants used in folk medicine," De Pharmazie 2009;64(4):260-268.
26. Al-Oqail MM, Al-Sheddi ES, Siddiqui MA, Musarrat J, Al-Khedhairy AA, Farshori NN. "Anticancer activity of chloroform extract and sub fractions of *P. amboinicus* on human breast and lung cancer cells: an *in vitro* cytotoxicity assessment," Pharmacognosy Magazine 2015;11(44):598-605.
27. M. A. Siddiqui, M. P. Kashyap, V. Kumar, A. A. Al-Khedhairy, J. Musarrat, and A. B. Pant, "Protective potential of transresveratrol against 4-hydroxynonenal induced damage in PC12 cells," Toxicology *in vitro*, vol. 24, no. 6, pp. 1592–1598, 2010.
28. M. A. Siddiqui, H. A. Alhadlaq, J. Ahmad, A. A. Al-Khedhairy, J. Musarrat, and M. Ahamed, "Copper oxide nanoparticles induced mitochondria mediated apoptosis in human hepato carcinoma cells," PLoS ONE, vol. 8, no. 8, Article ID e69534, 2013.
29. Y. Zhang, L. Jiang, L. Jiang *et al*., "Possible involvement of oxidative stress in potassium bromate-induced genotoxicity in human hepG2 cells," Chemico-Biological Interactions 2011;189(3):186-191.
30. Saquib Q, Al-Khedhairy AA, Siddiqui MA, AbouTarboush FM, Azam A, Musarrat J. "Titanium dioxide nanoparticles induced cytotoxicity, oxidative stress and DNA damage in human amnion epithelial (WISH) cells," Toxicology *in vitro* 2012;26(2):351–361.
31. Saquib Q, Musarrat J, Siddiqui MA *et al*., "Cytotoxic and necrotic responses in human amniotic epithelial (WISH) cells exposed to organophosphate insecticide phorate," Mutation Research/Genetic Toxicology and Environmental Mutagenesis 2012;744(2):125-134.
32. Mulfinger L, Solomon SD, Bahadory M *et al*., "Biosynthesis and study of silver nanoparticles," Journal of Chemical Education 2007;84(2):322.
33. Sastry M, Mayyaa KS, Bandyopadhyay K. "pH dependent changes in the optical properties of carboxylic acid derivatized silver colloid particles," Colloids and Surfaces A: Physicochemical and Engineering Aspects, 1997;127(1-3):221-228.
34. Kelly KL, Coronado E, Zhao LL, Schatz GC. "The optical properties of metal nano particles: The influence of size, shape and dielectric environment," Journal of Physical Chemistry B 2003;107(3):668-677.
35. Rai A, Singh A, Ahmad A, Sastry M. "Role of halide ions and temperature on the morphology of biologically synthesized gold nanotriangles," Langmuir 2006;22(2):736-741.
36. El-Naggar NE, Abdelwahed NA, Darwesh OM. "Fabrication of biogenic antimicrobial silver nanoparticles by *streptomyces aegyptia* NEAE 102 as eco-friendly nano factory," Journal of Microbiology and Biotechnology 2014;24(4):453-464.
37. Jha AK, Prasad K, Kumar V, Prasad K. "Biosynthesis of silver nanoparticles using *Eclipta leaf*," Biotechnology Progress 2009;25(5):1476-1479.
38. Borchert H. "Determination of nanocrystal sizes: a comparison of TEM, SAXS, and XRD studies of highly monodisperse CoPt3 particles," Langmuir 2005;21(5):1931-1936.
39. Arunachalam KD, Arun LB, Annamalai SK, Arunachalam AM. "Potential anticancer properties of bioactive compounds of *Gymnema sylvestre* and its bio functionalized silver nanoparticle," International Journal of Nanomedicine 2015;10:31-41.
40. Kumar PV, Pammi SVN, Kollu P, Satyanarayana KVV, Shameem U. " biosynthesis and characterization of silver nanoparticles using *Boerha aviadiffusa* plant extract and their anti bacterial activity," Industrial Crops and Products 2014;52:562-566.

41. Mallikarjuna K, Sushma NJ, Narasimha G, Manoj L, Raju BDP. "Phytochemical fabrication and characterization of silver nanoparticles by using *pepper* leaf broth," Arabian Journal of Chemistry 2014;7(6):1099-1103.
42. Nogueira DR, Mitjans M, Infante MR, Vinardell MP. "Comparative sensitivity of tumor and nontumor cell lines as a reliable approach for *in vitro* cytotoxicity screening of lysine-based surfactants with potential pharmaceutical applications," International Journal of Pharmaceutics 2011;420(1):51-58.
43. Mosmann T. "Rapid colorimetric assay for cellular growth and survival: application to proliferation and cytotoxicity assays," Journal of Immunological Methods, 1983;65(1-2):55-63.
44. Borenfreund E, Puerner JA. "Short-term quantitative *in vitro* cytotoxicity assay involving an S-9 activating system," Cancer Letters 1987;34(3):243-248.
45. Farah MA, Ali MA, Chen SM *et al*., "Silver nanoparticles synthesized from *adenium obesum* leaf extract induced DNA damage, apoptosis and autophagy via generation of reactive oxygen species," Colloids and Surfaces B: Biointerfaces 2016;141:158-169.
46. Vivek R, -angam R, Muthuchelian K, Gunasekaran P, Kaveri K, Kannan S. "biosynthesis of silver nanoparticles from *Annona squamosa* leaf extract and it's *in vitro* cytotoxic effect on MCF-7 cells," Process Biochemistry, 2012;47(12):2405-2410.
47. Jacob SJP, Finub JS, Narayanan A. "Biosynthesis of silver nanoparticles using *piper longum* leaf extracts and its cytotoxic activity against Hep-2 cell line," Colloids and Surfaces B: Biointerfaces 2012;91:212-214.
48. Suman TY, Rajasree SR, Kanchana A, Elizabeth SB. "Biobiosynthesis, characterization and cytotoxic effect of plant mediated silver nanoparticles using *Morinda citrifolia* root extract," Colloids and Surfaces B: Biointerfaces 2013;106:74-78.
49. Siddiqui MA, Saquib Q, Ahamed M *et al*., "Molybdenum nanoparticles-induced cytotoxicity, oxidative stress, G2/M arrest, and DNA damage in mouse skin fibroblast cells (L929)," Colloids and Surfaces B: Biointerfaces 2015;125:73-81.
50. El-Sonbaty SM. "Fungus-mediated biosynthesis of silver nanoparticles and evaluation of antitumor activity," Cancer Nanotechnology 2013;4(4-5):73-79.
51. Soenen SJ, De Cuyper M. "Assessing cytotoxicity of (iron oxide-based) nanoparticles: an overview of different methods exemplified with cationic magnetoliposomes," Contrast Media and Molecular Imaging 2009;4(5):207–219.
52. Stroh A, Zimmer C, Gutzeit C *et al*., "Iron oxide particles for molecular magnetic resonance imaging cause transient oxidative stress in rat macrophages," Free Radical Biology and Medicine 2004;36(8):976-984.
53. Dwivedi S, Siddiqui MA, Farshori NN, Ahamed M, Musarrat J, Al-Khedhairy AA. "Biosynthesis, characterization and toxicological evaluation of iron oxide nanoparticles in human lung alveolar epithelial cells," Colloids and Surfaces B: Biointerfaces 2014;122:209-215.
54. Nicoletti I, Migliorati G, Pagliacci MC, Grignani F, Riccardi C. "A rapid and simple method for measuring thymocyte apoptosis by propidium iodide staining and flow cytometry," Journal of Immunological Methods, 1991;139(2):271-279.
55. Ravi S, Chiruvella KK, Rajesh K, Prabhu V, Raghavan SC. "5-isopropylidene-3-ethylrhodanine induce growth inhibition followed by apoptosis in leukemia cells," European Journal of Medicinal Chemistry 2010;45(7):2748-2752.
56. Asharani PV, Hande MP, Valiyaveettil S. "Antiproliferative activity of silver nanoparticles," BMC Cell Biology 2009;10(1):65-79.
57. Ciftci H, Turk M, Tamer U, Karahan S, Menemen Y. "Silver nanoparticles: cytotoxic, apoptotic, and necrotic effects on MCF-7 cells," Turkish Journal of Biology 2013;37:573-581.
58. Foldbjerg R, Olesen P, Hougaard M, Dang DA, Hoffmann HJ, Autrup H. "PVP-coated silver nanoparticles and silver ions induce reactive oxygen species, apoptosis, and necrosis in THP-1 monocytes," Toxicology Letters 2009;190(2):156-162.
59. Hsin YH, Chen CF, Huang S, Shih TS, Lai PS, Chueh PJ. "The apoptotic effect of nanosilver is mediated by a ROS-and JNK-dependent mechanism involving the mitochondrial pathway in NIH3T3 cells," Toxicology Letters 2008;179(3):130-139.
60. Pan Y, Neuss S, Leifert A *et al*., "Size-dependent cytotoxicity of gold nanoparticles," Small 2007;3(11):1941-1949.